JACS
JOURNAL OF THE AMERICAN CHEMICAL SOCIETY
Article
pubs.acs.org/JACS

A "Smart" ^{129}Xe NMR Biosensor for pH-Dependent Cell Labeling

Brittany A. Riggle, Yanfei Wang, and Ivan J. Dmochowski*

Department of Chemistry, University of Pennsylvania, 231 South 34th Street, Philadelphia, Pennsylvania 19104-6323, United States

Supporting Information

ABSTRACT: Here we present a "smart" xenon-129 NMR biosensor that undergoes a peptide conformational change and labels cells in acidic environments. To a cryptophane host molecule with high Xe affinity, we conjugated a 30mer EALA-repeat peptide that is α-helical at pH 5.5 and disordered at pH 7.5. The ^{129}Xe NMR chemical shift at room temperature was strongly pH-dependent ($\Delta\delta$ = 3.4 ppm): δ = 64.2 ppm at pH 7.5 vs δ = 67.6 ppm at pH 5.5, where Trp(peptide)−cryptophane interactions were evidenced by Trp fluorescence quenching. Using hyper-CEST NMR, we probed peptidocryptophane detection limits at low-picomolar (10^{-11} M) concentration, which compares favorably to other NMR pH reporters at 10^{-2}−10^{-3} M. Finally, in biosensor-HeLa cell solutions, peptide−cell membrane insertion at pH 5.5 generated a 13.4 ppm downfield cryptophane-^{129}Xe NMR chemical shift relative to pH 7.5 studies. This highlights new uses for ^{129}Xe as an ultrasensitive probe of peptide structure and function, along with potential applications for pH-dependent cell labeling in cancer diagnosis and treatment.

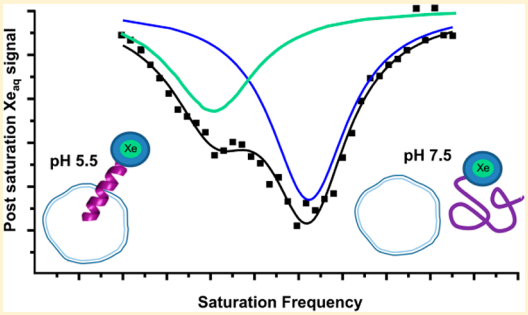

INTRODUCTION

Magnetic resonance imaging (MRI) and spectroscopy (MRS) are versatile and commonly employed techniques for the diagnosis and staging of disease.[1] The development of targeted and stimuli-responsive (i.e., "smart") contrast agents improves the capabilities of MRI/MRS for molecular imaging.[2] Targeted therapeutic and diagnostic imaging techniques are typically directed to one or more receptors associated with a disease state. However, in cancer, as a result of large natural variations between cells and the heterogeneous nature of tissue within a tumor, there is also need for more general biomarkers.[3,4] For example, hypoxia and acidification occur in 90% of tumors and are key microenvironmental factors in progression and treatment resistance in solid tumors.[5,6] The tumor microenvironment is acidified to levels approaching pH 6.0 from a normal pH of 7.4, which increases metastasis, mutation rate, and cell viability.[4,7−9] Therefore, being able to identify cells in acidic environments has practical importance in the design of cancer therapies and controlled-release drug delivery mechanisms.[8] In addition, acidic environments can mitigate the efficacy of weakly basic chemotherapeutics, such as doxorubicin, necessitating methodologies to probe extracellular pH (pH$_e$).[10] Here, we present an ultrasensitive xenon-based MR contrast agent that can identify and label cell populations on the basis of their acidic pH$_e$.

A variety of pH-responsive MR contrast agents have been designed previously, including Gd complexes,[11,12] tunable micelle-encapsulated polymers and ^{19}F compounds,[13,14] and CEST agents,[15−21] among others.[22,23] These probes enable measurements of solution pH but do not selectively label cells in acidic environments, for example, as needed for identifying small populations of cancer cells or performing cell tracking experiments. In parallel efforts over the past two decades, many strategies have been developed for labeling cells with MRI contrast agents such as membrane-targeting Gd chelates, monocrystalline iron oxide particles (MIONs),[25] micrometer-sized iron oxide particles (MPIOs),[26] ultrasmall dextran-coated iron oxide particles (USPIOs),[27] and superparamagnetic iron oxide (SPIO) glycol chitosan.[9,28] Pioneering studies by the Tsourkas lab and others have explored pH-dependent cell labeling with these reagents, but there remain significant limitations, for example, pH-responsive SPIO typically requires significant incubation time (~24 h) between administration and imaging.[9] More generally, applications with conventional MRI contrast agents are limited by low detection sensitivity on a per-monomer basis (i.e., low millimolar). One strategy for improving NMR detection sensitivity involves the use of exogenously supplied "hyperpolarized" (hp) nuclei, for example, ^{129}Xe, ^{13}C, and ^{3}He, with magnetic spin reservoirs that exceed the normal Boltzmann distribution by several orders of magnitude. Xe binds void spaces in materials,[29] proteins,[30] and spores[31] but shows highest affinity and useful exchange kinetics for a class of host molecules known as cryptophane.[32−39] Perturbation of the large (~42 Å^3 volume) ^{129}Xe electron cloud can produce significant nuclear magnetic chemical shift changes and results in a nearly 300 ppm chemical shift window when bound to different cryptophanes in aqueous solution.[33,40,41]

On the basis of these principles, we and others have developed ^{129}Xe-cryptophane NMR biosensors[42] for the sensitive detection of protein receptors,[42−46] enzymes,[47]

Received: February 22, 2015
Published: April 7, 2015

DOI: 10.1021/jacs.5b01938
J. Am. Chem. Soc. 2015, 137, 5542−5548

DNA,[48] and metal ions in solution.[49] In one proof-of-concept experiment, Berthault et al. decorated cryptophane with six carboxylic acids to create a pH reporter: unique chemical shifts were measured over the pH 3.5−5.5 range with a total $\Delta\delta$ of 3.55 ppm.[50] However, solubility issues precluded work near neutral pH.

Recent studies have moved xenon biosensing from buffer solutions to lipid membrane suspensions and living cells. The Pines group developed ultrasensitive methods for detecting cryptophane in solution using hp ^{129}Xe chemical exchange saturation transfer (hyper-CEST) NMR spectroscopy.[51] They also discovered that cryptophane in association with a dilute suspension of submicrometer Intralipid vesicles yielded a ^{129}Xe NMR peak that was shifted ∼10 ppm downfield from the aqueous ^{129}Xe-cryptophane peak;[52] similar results were later obtained with different lipid compositions.[53] The Schröder lab subsequently performed hyper-CEST NMR spectroscopy and imaging studies in cells loaded with lipophilic cryptophane and found a similar 9−11 ppm downfield chemical shift change, likely due to membrane association.[54−56] These studies highlight the large ^{129}Xe NMR chemical shift changes that can be achieved by engineering cryptophane-lipid membrane interactions.

Building on these examples, we set out to develop an ultrasensitive ^{129}Xe NMR contrast agent for labeling cells in acidic microenvironments. Recent work from our laboratory[57] and elsewhere[58,59] has demonstrated nanomolar-to-picomolar detection of water-soluble cryptophane using hyper-CEST NMR spectroscopy. Most recently, Witte et al. demonstrated effective contrast via hyper-CEST by site-specific labeling of cell-surface glycans with nanomolar concentrations of cryptophane.[60] Thus, hyper-CEST NMR should enable ultrasensitive detection of cryptophane-labeled cells that reside in acidic environments and differentiation from "normal" cells residing in neutral pH environments, provided that cryptophane−cell interactions can be modulated over the pH range 5.5−7.5.

We hypothesized that modifying cryptophane with an EALA-repeat peptide, WEAALAEALAEALAEHLAEALAEALEALAA,[61] should modulate ^{129}Xe NMR chemical shift in response to physiologic pH changes. By our strategy, the ^{129}Xe NMR chemical shift should vary from both pH-dependent peptide conformational changes as well as pH-dependent peptido-cryptophane-cell membrane association. The synthetic EALA-repeat peptide was inspired originally by hemaglutinin, which membrane inserts in low-pH environments.[61] The poly-(glutamic acid) nature of the EALA-repeat peptide elevates the pK_a to around 6, resulting in a conformational change from random coil (pH 7.5) to mostly α-helical (pH 5.5), over a biologically relevant pH range.[62] As the glutamates are protonated, the EALA-repeat peptide becomes more helical and hydrophobic, and it inserts into lipophilic membranes.[63] This pH-dependent membrane insertion has been used in living cells to facilitate endosomal escape of both nanocapsule and gene payloads.[64−66] Thus, by appending cryptophane to a membrane-inserting EALA peptide, we endeavored to generate a xenon contrast agent capable of being "activated" in acidic cell environments to label cell membranes and give large ^{129}Xe NMR chemical shift changes. We based the design on our previously reported tripropargyl cryptophane-A derivative (with two cyclotriveratrylene units tethered by three ethylene linkers),[67] which should allow facile attachment of a pH-responsive peptide and also two water-solubilizing moieties (Scheme 1) to mitigate the potential for cryptophane aggregation.[55]

Scheme 1. Synthesis of Water-Soluble EALA-Cryptophane (WEC)[a]

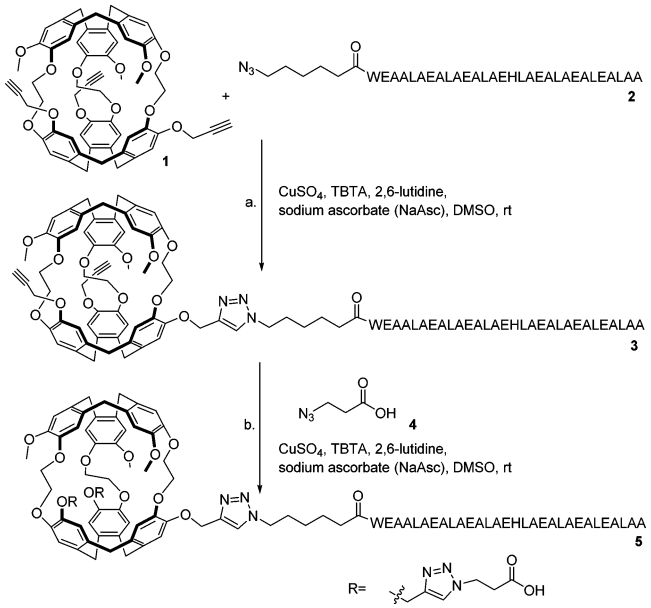

[a](a) 1 (1 equiv), 2 (1 equiv), $CuSO_4$ (1 equiv), TBTA (5 equiv), 2,6-lutidine (1 equiv), NaAsc (10 equiv), 12 h. (b) 3 (crude), 4 (10 equiv), $CuSO_4$ (1 equiv), TBTA (5 equiv), 2,6-lutidine (1 equiv), NaAsc (10 equiv), 12 h.

RESULTS AND DISCUSSION

Synthetic Procedures. Scheme 1 shows the synthesis of the water-soluble EALA-cryptophane (WEC) pH-responsive biosensor **5**, the details of which are provided in the Supporting Information (SI). Briefly, the synthesis of tripropargyl cryptophane **1** was performed in six nonlinear steps with modifications to previously published methods,[68] with an overall yield of 6.4% (SI Scheme S1). The yield for the five linear steps was 9.9%. The azido-EALA-repeat peptide **2** was prepared with standard Fmoc synthetic methods (SI Figures S1, S2). The peptide was attached to the cryptophane via copper(I)-catalyzed [3 + 2] azide−alkyne cycloaddition (CuAAC) to form **3**.[69,70] The monopeptide cryptophane was preferentially achieved by controlling the reaction stoichiometry. The resulting triazole-hexyl spacer kept the peptide in close proximity to the ^{129}Xe nucleus while minimizing steric clashes with cryptophane during conjugation. Formation of compound **3** was confirmed by MALDI-MS, and the yield was quantified by analytical reversed-phase HPLC to be 60−80% (SI Figures S3, S4). A solubilizing linker, 3-azidopropionic acid **4**, was synthesized in one step from the commercially available β-propiolactone (see Supporting Information)[47,71] and reacted with crude **3** via a second CuAAC. Starting from tripropargyl cryptophane **1**, WEC **5** was isolated in ∼40% yield after sequential CuAAC reactions with **2** and **4** and HPLC purification to remove unreacted EALA peptide and unreacted cryptophane (SI Figures S5, S6).

Electronic Circular Dichroism (ECD) Spectroscopy. For ECD studies, all samples of azidopeptide **2** or WEC were prepared at 30 μM concentration in 10 mM sodium phosphate

DOI: 10.1021/jacs.5b01938
J. Am. Chem. Soc. 2015, 137, 5542−5548

buffer, as confirmed by UV−vis spectroscopy (peptide: ε_{280} = 5700 M^{-1} cm^{-1}, WEC: ε_{280} = 17 700 M^{-1} cm^{-1}) and pH-adjusted with 1 M HCl or 1 M NaOH. We used ECD spectroscopy to confirm that azidopeptide **2** maintained pH sensitivity (Figure 1a):[61,72,73] indeed, the percent helicity

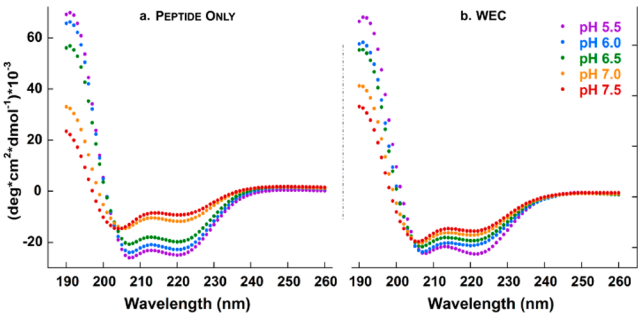

Figure 1. pH titrations monitored by ECD spectroscopy for (a) azido-EALA peptide and (b) water-soluble EALA-cryptophane (WEC). Samples (30 μM) were in 10 mM sodium phosphate buffer over the pH range 5.5−7.5 at 298 K.

increased from 25% to 67% as the pH was decreased from 7.5 to 5.5 (SI Table S1). The ECD signal at pH 5.5 had pronounced local minima at 208 and 222 nm, indicative of an α-helical secondary structure. At pH 7.5, the spectrum approached a minimum at 204 nm while subsequently decreasing in negative ellipticity at 222 nm, which is characteristic of a more disordered state. For the WEC (Figure 1b, SI Figure S7), we observed a similar increase in EALA helicity from 36% (pH 7.5) to 61% (pH 5.5). These data established that the peptide still undergoes a significant conformational change when conjugated to the cryptophane. Samples showed reproducible and reversible secondary structure changes between pH 5.5 and 7.5 (SI Figure S8). Interestingly, WEC was more ordered at pH 7.5 than peptide alone, suggesting that the cryptophane elevated the conjugated peptide pK_a. Similar pK_a elevation was previously observed for the analogous tris-propionic acid cryptophane as a result of the bulky, hydrophobic cryptophane disfavoring ionization of the nearby propionates.[35]

Tryptophan Fluorescence. The EALA-repeat peptide contains a single N-terminal tryptophan that we hypothesized should provide a useful local probe of peptide conformation, as well as peptide−cryptophane interaction. Fluorescence studies (λ_{ex} = 280 nm) with peptide **2** demonstrated blue-shifted and somewhat quenched Trp emission with decreasing pH: 352 nm (pH 7.5) to 343 nm (pH 5.5) (Figure 2a). Trp maximum emission wavelength for the WEC decreased from 336 to 322 nm over the same pH range (Figure 2b), which was considerably blue-shifted relative to peptide **2** alone, which is consistent with the Trp experiencing a less solvated environment near cryptophane. We note that the fluorescence signal for the amino acid tryptophan is typically not perturbed by pH changes in the range of 4−8,[74] whereas Trp incorporated within peptides can exhibit emission that is very sensitive to the peptide folded state.

Cryptophane fluoresces (λ_{max} = 313 nm) with an intensity comparable to that of Trp, which further blue-shifts the observed emission spectrum.[35,44] At all pH values, cryptophane quenched Trp emission, as compared with the free peptide (Figure 2c). Plots of F/F_0 vs pH (Figure 2c, where F is the fluorescence emission at a given pH and F_0 is the maximal

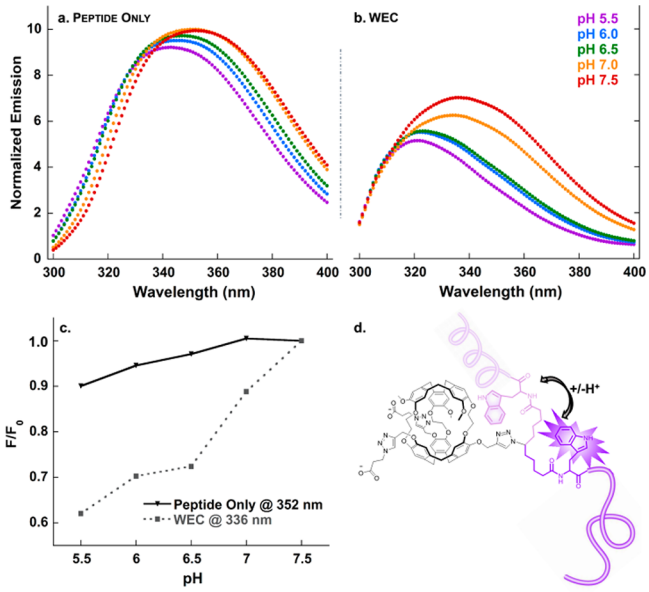

Figure 2. pH titration monitored by Trp fluorescence for (a) azido-EALA peptide; (b) water-soluble EALA-cryptophane (WEC); (c) plot of F/F_0 for the λ_{max} of peptide only (352 nm) and WEC (336 nm) as a function of pH; and (d) representation of α-helical and disordered peptide(Trp)−cryptophane interaction. Samples (30 μM) were in 10 mM sodium phosphate buffer over the pH range 5.5−7.5 at 298 K.

fluorescence emission at pH 7.5) confirmed that cryptophane quenching increased from pH 7.5 down to pH 5.5, where cryptophane−Trp interactions were presumably more prevalent with the relatively uncharged, α-helical peptide. This analysis is in agreement with an earlier work with a peptide−cryptophane conjugate for which we examined the interaction between the Trp-containing peptide and cryptophane with a temperature-dependent quenching assay and Stern−Volmer analysis.[44] These experiments revealed that Trp(peptide)−cryptophane complex formation resulted in a loss of Trp fluorescence. Previous studies identified high-affinity interactions between C_{60} (an aromatic molecule with dimensions and spherical shape similar to that of cryptophane) and Trp-containing proteins, which also resulted in Trp fluorescence quenching and blue-shifted emission.[75−77] These results support a mechanism by which the EALA peptide can mediate Trp−cryptophane complex formation in WEC (Figure 2d) and result in pH-dependent Trp fluorescence quenching. Importantly, Trp−cryptophane π-stacking interactions have the potential to deshield ^{129}Xe within the cryptophane cavity and produce a downfield chemical shift.[78−80]

^{129}Xe NMR Spectroscopy. We initially performed hp ^{129}Xe NMR studies to examine the sensitivity of the cryptophane-encapsulated ^{129}Xe chemical shift to the nearby peptide conformational state. NMR samples were identically prepared at 30 μM concentrations in 10 mM sodium phosphate buffer. Repeated trials at 300 ± 1 K ([Xe] = 6.2 mM)[81] with the WEC at pH 7.5, 6.5, and 5.5 gave reproducible chemical shifts (Figure 3). A single peak was observed at both pH 5.5 (67.6 ± 0.5 ppm) and pH 7.5 (64.2 ± 0.5 ppm), with a chemical shift difference of 3.4 ppm. Interestingly, although the cryptophane itself is a racemic mixture of stereoisomers and the EALA-repeat peptide is chiral, we did not observe a pair of diastereomeric peaks at pH 7.5 or pH 5.5, as we reported for previous peptide−cryptophane xenon biosensors[44,45] and has

DOI: 10.1021/jacs.5b01938
J. Am. Chem. Soc. 2015, 137, 5542−5548

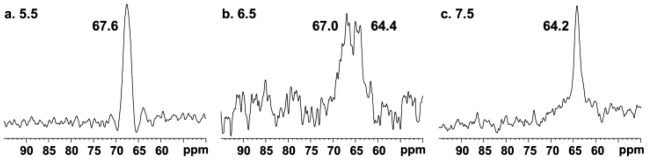

Figure 3. hp^{129}Xe NMR spectra (average of 16 scans, line-broadening = 60 Hz) of WEC (30 μM) in 10 mM sodium phosphate buffer at 300 ± 1 K, with peak widths (fwhm) indicated in Hz: (a) pH 5.5, 211 Hz; (b) pH 6.5, 317, and 214 Hz; (c) pH 7.5, 154 Hz.

been seen for various racemic xenon biosensors complexed to protein active sites.[49] We hypothesize that the two diastereomers provide a very similar environment for the bound xenon atom and produce what appears to be a single ^{129}Xe NMR peak at both pH values. In this case, the inclusion of solubilizing propionates promotes open, xenon-binding conformations of the cryptophane, regardless of peptide conformation. Conversely, the equal-intensity peaks observed at pH 6.5 (δ = 67.0 and 64.4 ppm) may result from hp^{129}Xe experiencing very different environments within the two WEC diastereomers.

Hyper-CEST ^{129}Xe NMR. To improve detection sensitivity of WEC over direct detection by nearly 6 orders of magnitude, we employed hyper-CEST NMR spectroscopy. This indirect detection method took advantage of the exchanging ^{129}Xe population between bulk aqueous solution and the xenon host molecule (Figure 4) by selectively saturating the bound signal

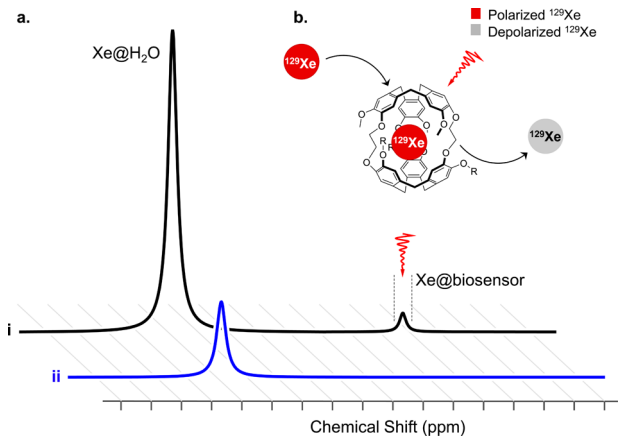

Figure 4. Hyper-CEST detection scheme for WEC-encapsulated ^{129}Xe. (a) Representative spectra are shown for (i) the initial spectrum and (ii) the resulting spectrum from selective "on resonance" saturation of the WEC-encapsulated ^{129}Xe and commensurate bulk ^{129}Xe@H$_2$O depolarization. (b) Selective radio frequency depolarization of WEC-encapsulated ^{129}Xe.

(Figure 4b). Because of xenon exchange, the selective depolarization resulted in a concomitant signal loss from the ^{129}Xe@water peak, which was readily monitored (Figure 4a). This signal was compared with a reference measurement in which an "off-resonance" saturation was applied to account for the natural self-relaxation of hp^{129}Xe@water over time.

Using 34pM WEC (pH 7.5, 310 K, [Xe] = 0.15 mM) indirect detection via hyper-CEST was performed by applying shaped radiofrequency saturation pulses at the ^{129}Xe@WEC resonance frequency and measuring the residual aqueous ^{129}Xe signal for different saturation duration (Figure 5). WEC was observed to "catalyze" this depolarization process through on-

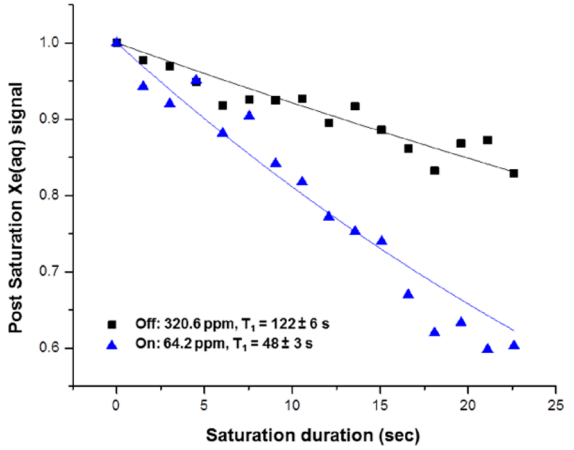

Figure 5. Hyper-CEST signal decay of 34 pM WEC at pH 7.5, 310 K. Depolarization rates were measured with radiofrequency pulses either on-resonance (64.2 ppm) or off-resonance (320.6 ppm) with hp^{129}Xe@WEC.

resonance (64.2 ppm) saturation rf pulses with ^{129}Xe@WEC in pH 7.5 buffer. In contrast, saturation pulses applied off-resonance (320.6 ppm) gave a depolarization time that approximated the natural T_1 of hp^{129}Xe in water.

We also investigated the pH sensitivity of WEC-hp^{129}Xe NMR chemical shift to look at "normal" (pH 7.5) and acidic (pH 5.9) buffer solutions (Figure 6). Because depolarization

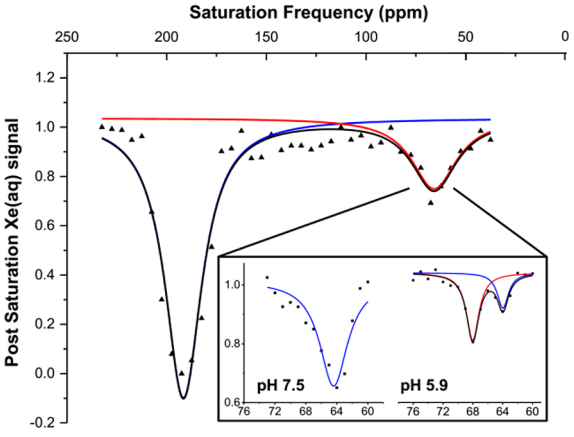

Figure 6. Hyper-CEST scan of WEC (1 μM) at 300 K. Full image was collected with 5 ppm step and individual peaks with 1 ppm step at pH 7.5 and pH 5.9 (inset).

efficiency is decreased with a narrower saturation pulse, WEC was employed at 1 μM concentrations, which is still at least 10^3-fold more dilute than demonstrated for ^{1}H CEST pH reporters.[82] Prior to detecting a free xenon signal, a loop of selective DSnob-shaped saturation pulses was scanned over the chemical shift range of 40−230 ppm in 5 ppm (700 Hz) steps, which corresponded to a pulse length of 3748.6 μs and power of 77 μT. Two saturation responses centered at 195 ppm (^{129}Xe@H$_2$O) and 65 ppm (^{129}Xe@WEC) were observed (Figure 6, full image). By decreasing the frequency scanning step size to 1 ppm (138.2 Hz), which corresponded to a shaped pulse length of 19014 μs and power of 15 μT, we were able to distinguish the WEC-encapsulated ^{129}Xe peak for pH 7.5 and pH 5.9 samples at 300 K (Figure 6, inset). The total time to record the hyper-CEST NMR spectra was composed of xenon

DOI: 10.1021/jacs.5b01938
J. Am. Chem. Soc. 2015, 137, 5542−5548

delivery time (20 s) and data collection time. For the latter, each data point required time T:

$$T = (\text{sp } 6 + d12)*L6 + d1 + p1$$

In the 5-ppm step scanning experiments, sp6 (saturation pulse length) = 3.748 ms, $d12$ (delay between saturation pulses) = 20 μs, L6 (number of saturation cycles) = 400, $d1$ (delay before acquisition pulse) = 0.5 s, $p1$ (acquisition pulse) = 22 μs. Thus, the total time needed to acquire the whole spectrumwas 860 s. In the 1 ppm step scanning experiments, sp6 = 19.014 ms, $L6$ = 600, and the total time needed was 478 s. The observed pair of peaks at pH 5.9 was similar to hp^{129}Xe NMR data collected for 30 μM WEC by direct detection at pH 6.5 (Figure 3). As illustrated by these data, the hyper-CEST ^{129}Xe NMR spectrum readily distinguished between physiologically normal and acidic pH values.

Cellular Hyper-CEST ^{129}Xe NMR. Finally, we investigated the utility of WEC in a biological setting through ^{129}Xe NMR cell studies. Human cervical carcinoma (HeLa) cells were grown in a flask to confluency. Cells were washed and suspended in either pH 7.5 or 5.5 sodium phosphate buffer containing 5−10 μM WEC to give 1 × 10^7 cells/mL concentrations. Pluronic L-81 (0.1% final concentration) was added to reduce foaming that can result from Xe bubbling.[54] Cells were incubated under these conditions for 45−60 min and then transferred to an NMR tube. Spectra were acquired at both pH values, with a frequency scanning step size of 1 ppm (138.2 Hz), 400 cycles, which corresponded to a shaped pulse length of 19014 μs and power of 15 μT. Figure 7a shows xenon in cells (196.3 ppm, red trace) and xenon dissolved in aqueous solution of HeLa cells suspended in pH 7.5 buffer with WEC (192.3 ppm, blue trace). Figure 7b shows WEC-encapsulated xenon in the same sample. ^{129}Xe@WEC$_{aq}$, pH 7.5, gave a chemical shift of 65.0 ppm, which corresponds to a free biosensor in buffer at pH 7.5. In pH 5.5 experiments, Figure 7c shows two peaks, one for Xe@cells (198.0 ppm, red trace) and one for Xe@aq (192.0 ppm, blue trace). Figure 7d shows the biosensor region of the same sample and exhibits two peaks, one at 68.0 ppm corresponding to free α-helical WEC in buffer (blue trace) and one at 78.4 ppm that we assign to WEC inserted in the cell membrane (red trace). Notably, upon biosensor-membrane insertion at pH 5.5, we observed a 13.4 ppm downfield chemical shift compared with biosensor-cell solutions at pH 7.5. Contrary to previous ^{129}Xe NMR cell studies performed with a more lipophilic cryptophane, we did not observe cryptophane−membrane association at pH 7.5.[52] This result is also consistent with previous studies with the EALA peptide that showed no membrane association at pH 7.5.[83] By targeting the acidic pH$_e$ as a general cancer biomarker, along with membrane association, we increased the chemical shift difference between Xe@biosensor$_{cells}$ and Xe@biosensor$_{aq}$ as compared with earlier studies.[53−55] We note that in living organisms, there will be additional factors (beyond pH$_e$) that impact the ^{129}Xe@biosensor$_{cells}$ chemical shift, including cell type and membrane composition. Follow-up studies will be required to assess this variability.

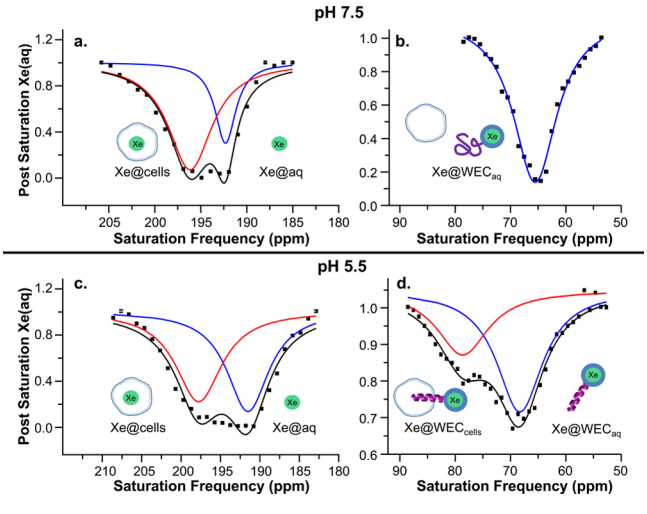

Figure 7. Hyper-CEST ^{129}Xe NMR spectra for 5−10 μM WEC in 10 mM sodium phosphate buffer with 0.1% Pluronic L-81 in a suspension of 1 × 10^7 cells/mL. Data were collected at pH 7.5 (a) Xe@cells, red trace (196.3 ppm); Xe@aq, blue trace (192.3 ppm); (b) Xe@WEC$_{aq}$ (65.0 ppm) and at pH 5.5; (c) Xe@cells, red trace (198.0 ppm); Xe@aq, blue trace (192.0 ppm); (d) Xe@WEC$_{cells}$, red trace (78.4 ppm) and Xe@WEC$_{aq}$, blue trace (68.0 ppm). Exponential Lorentzian fits are shown as colored solid lines, and the corresponding sums are shown as solid black lines.

CONCLUSIONS

In summary, by attaching a pH-responsive, membrane-inserting peptide and two water-solubilizing moieties to a tripropargyl cryptophane host, we were able to generate an ultrasensitive ^{129}Xe NMR biosensor capable of labeling cells in acidic microenvironments. This xenon biosensor is unique for undergoing a rapid and reversible conformational change (over a range of physiologic pH values) as well as functional changes: at pH 5.5, the pendant EALA-repeat peptide was mostly α-helical and gained membrane-insertion capabilities. This represents a "smart" ^{129}Xe MR contrast agent, and builds on previous examples of xenon biosensors that bind specific targets (e.g., protein receptors, DNA, cell-surface glycans) or undergo a modification event (i.e., enzyme-mediated peptide cleavage).

Significantly, this study demonstrated that appending the peptide to the ∼1-nm-diameter, hydrophobic cryptophane did not significantly reduce its ability to undergo a conformational change. Circular dichroism, Trp fluorescence, and hp ^{129}Xe NMR spectroscopies were employed to measure the change in helical character of the peptide in the pH range 5.5−7.5. EALA peptide helix formation resulted in a ^{129}Xe NMR downfield chemical shift change of 3.4 ppm, which was likely enhanced by significant cryptophane interactions with the nearby N-terminal Trp residue. This suggests a general strategy for engineering larger chemical shift changes with xenon biosensors, particularly to monitor molecular events occurring nanometers away from the xenon−cryptophane reporter. These data represent a significant advance over the previous example of a peptido-cryptophane biosensor, which monitored MMP-7 activity: only a 0.5 ppm chemical shift change was observed upon enzyme-mediated peptide cleavage, perhaps because the Trp was positioned much farther from the cryptophane.[44] For some in vivo applications, it may be useful to maintain the full range of pH-dependent conformational changes of the EALA-repeat peptide, and it will be interesting to explore different peptides and conjugation strategies that work to achieve this goal.

The design of a cryptophane−EALA peptide conjugate capable of membrane insertion at acidic pH advances our long-range goal of developing ultrasensitive ^{129}Xe MR contrast agents to aid in cancer diagnosis and treatment.[63,73] Picomolar

DOI: 10.1021/jacs.5b01938
J. Am. Chem. Soc. 2015, 137, 5542−5548

(10^{-11} M) concentrations of WEC were detected by hyper-CEST NMR, making this approach 8−9 orders of magnitude more sensitive than commonly employed MR contrast agents. We demonstrated a 13.4 ppm downfield chemical shift change from a disordered-peptide biosensor at pH 7.5 to the helical, membrane-inserted biosensor at pH 5.5. This represents the largest chemical shift change that has been engineered to date for a ^{129}Xe@cryptophane−biomolecule interaction, the magnitude of which should facilitate multiplexed detection in many experimental formats. The development and cellular implementation of this "smart" xenon biosensor are important steps toward future biomedical applications.

■ ASSOCIATED CONTENT

Supporting Information

Experimental and characterization details, including HPLC analysis and MALDI-MS data for biosensor and precursors. This material is available free of charge via the Internet at http://pubs.acs.org.

■ AUTHOR INFORMATION

Corresponding Author

*ivandmo@sas.upenn.edu

Notes

The authors declare no competing financial interest.

■ ACKNOWLEDGMENTS

This research was supported by NIH R01-GM097478, CDMRP-LCRP Concept Award No. LC130824, and GM097478S1 for 795 nm laser purchase. We thank Dr. Rakesh Kohli for assistance with MALDI-MS (supported by NSF MRI-0820996). We thank Drs. George Furst and Jun Gu for assistance with NMR spectroscopy. We thank Dr. E. James Petersson for use of a fluorometer. We also thank Dr. Christopher Lanci of the University of Pennsylvania Biological Chemistry Resource Center for automated peptide synthesis supported by UPenn Laboratory for Research on the Structure of Matter (NSF MRSEC DMR 0520020, 1120901). Dr. Jacob Goldberg provided assistance with CD spectroscopy. We thank Dr. Rebecca Wissner for synthetic advice, Judith Currano and Sean Yeldell for editorial assistance.

■ REFERENCES

(1) Caravan, P. *Chem. Soc. Rev.* **2006**, *35*, 512−523.
(2) Shao, H. L.; Yoon, T. J.; Liong, M.; Weissleder, R.; Lee, H. *Beilstein J. Nanotechnol.* **2010**, *1*, 142−154.
(3) An, M.; Wijesinghe, D.; Andreev, O. A.; Reshetnyak, Y. K.; Engelman, D. M. *Proc. Natl. Acad. Sci. U.S.A.* **2010**, *107*, 20246−20250.
(4) Thevenin, D.; An, M.; Engelman, D. M. *Chem. Biol.* **2009**, *16*, 754−762.
(5) Vavere, A. L.; Biddlecombe, G. B.; Spees, W. M.; Garbow, J. R.; Wijesinghe, D.; Andreev, O. A.; Engelman, D. M.; Reshetnyak, Y. K.; Lewis, J. S. *Cancer Res.* **2009**, *69*, 4510−4516.
(6) Andreev, O. A.; Engelman, D. M.; Reshetnyak, Y. K. *Mol. Membr. Biol.* **2010**, *27*, 341−352.
(7) Gillies, R. J.; Raghunand, N.; Garcia-Martin, M. L.; Gatenby, R. A. *IEEE Eng. Med. Biol. Mag.* **2004**, *23*, 57−64.
(8) Lee, E. S.; Gao, Z. G.; Bae, Y. H. *J. Controlled Release* **2008**, *132*, 164−170.
(9) Nwe, K.; Huang, C. H.; Tsourkas, A. *J. Med. Chem.* **2013**, *56*, 7862−7869.
(10) Gillies, R. J.; Raghunand, N.; Karczmar, G. S.; Bhujwalla, Z. M. *J. Magn. Reson. Imaging* **2002**, *16*, 430−450.
(11) Martinez, G. V.; Zhang, X. M.; Garcia-Martin, M. L.; Morse, D. L.; Woods, M.; Sherry, A. D.; Gillies, R. J. *NMR Biomed.* **2011**, *24*, 1380−1391.
(12) Garcia-Martin, M. L.; Martinez, G. V.; Raghunand, N.; Sherry, A. D.; Zhang, S. R.; Gillies, R. J. *Magn. Reson. Med.* **2006**, *55*, 309−315.
(13) Zhang, S. R.; Zhou, K. J.; Huang, G.; Takahashi, M.; Sherry, A. D.; Gao, J. M. *Chem. Commun.* **2013**, *49*, 6418−6420.
(14) Huang, X. N.; Huang, G.; Zhang, S. R.; Sagiyama, K.; Togao, O.; Ma, X. P.; Wang, Y. G.; Li, Y.; Soesbe, T. C.; Sumer, B. D.; Takahashi, M.; Sherry, A. D.; Gao, J. M. *Angew. Chem., Int. Ed.* **2013**, *52*, 8074−8078.
(15) Sheth, V. R.; Li, Y. G.; Chen, L. Q.; Howison, C. M.; Flask, C. A.; Pagel, M. D. *Magn. Reson. Med.* **2012**, *67*, 760−768.
(16) Zhang, S.; Merritt, M.; Woessner, D. E.; Lenkinski, R. E.; Sherry, A. D. *Acc. Chem. Res.* **2003**, *36*, 783−790.
(17) Dorazio, S. J.; Olatunde, A. O.; Tsitovich, P. B.; Morrow, J. R. *J. Biol. Inorg. Chem.* **2014**, *19*, 191−205.
(18) Hancu, I.; Dixon, W. T.; Woods, M.; Vinogradov, E.; Sherry, A. D.; Lenkinski, R. E. *Acta Radiol.* **2010**, *51*, 910−923.
(19) McMahon, M. T.; Gilad, A. A.; DeLiso, M. A.; Berman, S. M. C.; Bulte, J. W. M.; van Zijl, P. C. M. *Magn. Reson. Med.* **2008**, *60*, 803−812.
(20) Chan, K. W.; Yu, T.; Qiao, Y.; Liu, Q.; Yang, M.; Patel, H.; Liu, G.; Kinzler, K. W.; Vogelstein, B.; Bulte, J. W.; van Zijl, P. C.; Hanes, J.; Zhou, S.; McMahon, M. T. *J. Controlled Release* **2014**, *180*, 51−59.
(21) Longo, D. L.; Sun, P. Z.; Consolino, L.; Michelotti, F. C.; Uggeri, F.; Aime, S. *J. Am. Chem. Soc.* **2014**, *136*, 14333−14336.
(22) Gallagher, F. A.; Kettunen, M. I.; Brindle, K. M. *NMR Biomed.* **2011**, *24*, 1006−1015.
(23) Gallagher, F. A.; Kettunen, M. I.; Day, S. E.; Hu, D. E.; Ardenkjaer-Larsen, J. H.; in 't Zandt, R.; Jensen, P. R.; Karlsson, M.; Golman, K.; Lerche, M. H.; Brindle, K. M. *Nature* **2008**, *453*, 940−943.
(24) Carney, C. E.; MacRenaris, K. W.; Mastarone, D. J.; Kasjanski, D. R.; Hung, A. H.; Meade, T. J. *Bioconjugate Chem.* **2014**, *25*, 945−954.
(25) Weissleder, R.; Cheng, H. C.; Bogdanova, A.; Bogdanov, A. *J. Magn. Reson. Imaging* **1997**, *7*, 258−263.
(26) Shapiro, E. M.; Skrtic, S.; Sharer, K.; Hill, J. M.; Dunbar, C. E.; Koretsky, A. P. *Proc. Natl. Acad. Sci. U.S.A.* **2004**, *101*, 10901−10906.
(27) Bowen, C. V.; Zhang, X. W.; Saab, G.; Gareau, P. J.; Rutt, B. K. *Magn. Reson. Med.* **2002**, *48*, 52−61.
(28) Crayton, S. H.; Tsourkas, A. *ACS Nano* **2011**, *5*, 9592−9601.
(29) Xu, Y.; Tang, P. *BBA Biomembranes* **1997**, *1323*, 154−162.
(30) Rubin, S. M.; Lee, S. Y.; Ruiz, E. J.; Pines, A.; Wemmer, D. E. *J. Mol. Biol.* **2002**, *322*, 425−440.
(31) Bai, Y. B.; Wang, Y. F.; Goulian, M.; Driks, A.; Dmochowski, I. J. *Chem. Sci.* **2014**, *5*, 3197−3203.
(32) Kim, B. S.; Ko, Y. H.; Kim, Y.; Lee, H. J.; Selvapalam, N.; Lee, H. C.; Kim, K. *Chem. Commun.* **2008**, 2756−2758.
(33) Fogarty, H. A.; Berthault, P.; Brotin, T.; Huber, G.; Desvaux, H.; Dutasta, J. P. *J. Am. Chem. Soc.* **2007**, *129*, 10332−10333.
(34) Huber, G.; Brotin, T.; Dubois, L.; Desvaux, H.; Dutasta, J. P.; Berthault, P. *J. Am. Chem. Soc.* **2006**, *128*, 6239−6246.
(35) Hill, P. A.; Wei, Q.; Eckenhoff, R. G.; Dmochowski, I. J. *J. Am. Chem. Soc.* **2007**, *129*, 11662−11662.
(36) Hill, P. A.; Wei, Q.; Troxler, T.; Dmochowski, I. J. *J. Am. Chem. Soc.* **2009**, *131*, 3069−3077.
(37) Jacobson, D. R.; Khan, N. S.; Colle, R.; Fitzgerald, R.; Laureano-Perez, L.; Bai, Y.; Dmochowski, I. J. *Proc. Natl. Acad. Sci. U.S.A.* **2011**, *108*, 10969−10973.
(38) Taratula, O.; Kim, M. P.; Bai, Y. B.; Philbin, J. P.; Riggle, B. A.; Haase, D. N.; Dmochowski, I. J. *Org. Lett.* **2012**, *14*, 3580−3583.
(39) Taratula, O.; Yubin, B.; D'Antonio, E. L.; Dmochowski, I. J. *Supramol. Chem.* **2014**, *26*, 1−8.
(40) Raftery, D. *Annu. Rep. NMR Spectrosc.* **2006**, *57*, 205−270.
(41) Fairchild, R. M.; Joseph, A. I.; Holman, K. T.; Fogarty, H. A.; Brotin, T.; Dutasta, J. P.; Boutin, C.; Huber, G.; Berthault, P. *J. Am. Chem. Soc.* **2010**, *132*, 15505−15507.

DOI: 10.1021/jacs.5b01938
J. Am. Chem. Soc. 2015, 137, 5542−5548

(42) Spence, M. M.; Rubin, S. M.; Dimitrov, I. E.; Ruiz, E. J.; Wemmer, D. E.; Pines, A.; Yao, S. Q.; Tian, F.; Schultz, P. G. *Proc. Natl. Acad. Sci. U.S.A.* **2001**, *98*, 10654−10657.
(43) Seward, G. K.; Wei, Q.; Dmochowski, I. J. *Bioconjugate Chem.* **2008**, *19*, 2129−2135.
(44) Wei, Q.; Seward, G. K.; Hill, P. A.; Patton, B.; Dimitrov, I. E.; Kuzma, N. N.; Dmochowski, I. J. *J. Am. Chem. Soc.* **2006**, *128*, 13274−13283.
(45) Khan, N. S.; Riggle, B. A.; Seward, G. K.; Bai, Y.; Dmochowski, I. J. *Bioconjugate Chem.* **2015**, *26*, 101−109.
(46) Seward, G. K.; Bai, Y.; Khan, N. S.; Dmochowski, I. *Chem. Sci.* **2011**, *2*, 1103−1110.
(47) Chambers, J. M.; Hill, P. A.; Aaron, J. A.; Han, Z. H.; Christianson, D. W.; Kuzma, N. N.; Dmochowski, I. J. *J. Am. Chem. Soc.* **2009**, *131*, 563−569.
(48) Roy, V.; Brotin, T.; Dutasta, J. P.; Charles, M. H.; Delair, T.; Mallet, F.; Huber, G.; Desvaux, H.; Boulard, Y.; Berthault, P. *ChemPhysChem* **2007**, *8*, 2082−2085.
(49) Kotera, N.; Tassali, N.; Leonce, E.; Boutin, C.; Berthault, P.; Brotin, T.; Dutasta, J. P.; Delacour, L.; Traore, T.; Buisson, D. A.; Taran, F.; Coudert, S.; Rousseau, B. *Angew. Chem., Int. Ed. Engl.* **2012**, *51*, 4100−4103.
(50) Berthault, P.; Desvaux, H.; Wendlinger, T.; Gyejacquot, M.; Stopin, A.; Brotin, T.; Dutasta, J. P.; Boulard, Y. *Chem.—Eur. J.* **2010**, *16*, 12941−12946.
(51) Schröder, L.; Lowery, T. J.; Hilty, C.; Wemmer, D. E.; Pines, A. *Science* **2006**, *314*, 446−449.
(52) Meldrum, T.; Schröder, L.; Denger, P.; Wemmer, D. E.; Pines, A. *J. Magn. Reson.* **2010**, *205*, 242−246.
(53) Boutin, C.; Stopin, A.; Lenda, F.; Brotin, T.; Dutasta, J. P.; Jamin, N.; Sanson, A.; Boulard, Y.; Leteurtre, F.; Huber, G.; Bogaert-Buchmann, A.; Tassali, N.; Desvaux, H.; Carriere, M.; Berthault, P. *Biorg. Med. Chem.* **2011**, *19*, 4135−4143.
(54) Klippel, S.; Dopfert, J.; Jayapaul, J.; Kunth, M.; Rossella, F.; Schnurr, M.; Witte, C.; Freund, C.; Schröder, L. *Angew. Chem., Int. Ed.* **2014**, *53*, 493−496.
(55) Klippel, S.; Freund, C.; Schröder, L. *Nano Lett.* **2014**, *14*, 5721−5726.
(56) Sloniec, J.; Schnurr, M.; Witte, C.; Resch-Genger, U.; Schröder, L.; Hennig, A. *Chem.—Eur. J.* **2013**, *19*, 3110−3118.
(57) Bai, Y. B.; Hill, P. A.; Dmochowski, I. J. *Anal. Chem.* **2012**, *84*, 9935−9941.
(58) Meldrum, T.; Seim, K. L.; Bajaj, V. S.; Palaniappan, K. K.; Wu, W.; Francis, M. B.; Wemmer, D. E.; Pines, A. *J. Am. Chem. Soc.* **2010**, *132*, 5936−5937.
(59) Stevens, T. K.; Palaniappan, K. K.; Ramirez, R. M.; Francis, M. B.; Wemmer, D. E.; Pines, A. *Magn. Reson. Med.* **2013**, *69*, 1245−1252.
(60) Witte, C.; Martos, V.; Rose, H. M.; Reinke, S.; Klippel, S.; Schröder, L.; Hackenberger, C. P. R. *Angew. Chem., Int. Ed.* **2015**, *54*, 2806−2810.
(61) Subbarao, N. K.; Parente, R. A.; Szoka, F. C.; Nadasdi, L.; Pongracz, K. *Biochemistry* **1987**, *26*, 2964−2972.
(62) Nakaya, H. I.; Wrammert, J.; Lee, E. K.; Racioppi, L.; Marie-Kunze, S.; Haining, W. N.; Means, A. R.; Kasturi, S. P.; Khan, N.; Li, G. M.; McCausland, M.; Kanchan, V.; Kokko, K. E.; Li, S.; Elbein, R.; Mehta, A. K.; Aderem, A.; Subbarao, K.; Ahmed, R.; Pulendran, B. *Nat. Immunol.* **2011**, *12*, 786−795.
(63) Nicol, F.; Nir, S.; Szoka, F. C. *Biophys. J.* **1999**, *76*, 2121−2141.
(64) Nishimura, Y.; Takeda, K.; Ezawa, R.; Ishii, J.; Ogino, C.; Kondo, A. *J. Nanobiotechnol* **2014**, *12*, 1−6.
(65) Sasaki, K.; Kogure, K.; Chaki, S.; Nakamura, Y.; Moriguchi, R.; Hamada, H.; Danev, R.; Nagayama, K.; Futaki, S.; Harashima, H. *Anal. Bioanal. Chem.* **2008**, *391*, 2717−2727.
(66) Nouri, F. S.; Wang, X.; Dorrani, M.; Karjoo, Z.; Hatefi, A. *Biomacromolecules* **2013**, *14*, 2033−2040.
(67) Gabard, J.; Collet, A. *J. Chem. Soc., Chem. Commun.* **1981**, 1137−1139.
(68) Taratula, O.; Hill, P. A.; Bai, Y.; Khan, N. S.; Dmochowski, I. J. *Org. Lett.* **2011**, *13*, 1414−1417.
(69) Rostovtsev, V. V.; Green, L. G.; Fokin, V. V.; Sharpless, K. B. *Angew. Chem., Int. Ed.* **2002**, *41*, 2596−2599.
(70) Tornoe, C. W.; Christensen, C.; Meldal, M. *J. Org. Chem.* **2002**, *67*, 3057−3064.
(71) Seward, G. K.; Bai, Y.; Khan, N. S.; Dmochowski, I. *Chem. Sci.* **2011**, *2*, 1103−1110.
(72) Haas, D. H.; Murphy, R. M. *J. Pept. Res.* **2004**, *63*, 9−16.
(73) Li, W. J.; Nicol, F.; Szoka, F. C. *Adv. Drug Delivery Rev.* **2004**, *56*, 967−985.
(74) De Lauder, W. B.; Wahl, P. *Biochemistry* **1970**, *9*, 2750−2754.
(75) Song, M.; Liu, S.; Yin, J.; Wang, H. *Int. J. Mol. Sci.* **2011**, *12*, 4964−4974.
(76) Liu, S.; Sui, Y.; Guo, K.; Yin, Z.; Gao, X. *Nanoscale Res. Lett.* **2012**, *7*, 433−440.
(77) Belgorodsky, B.; Fadeev, L.; Ittah, V.; Benyamini, H.; Zelner, S.; Huppert, D.; Kotlyar, A. B.; Gozin, M. *Bioconjugate Chem.* **2005**, *16*, 1058−1062.
(78) Pelloni, S.; Lazzeretti, P.; Zanasi, R. *J. Phys. Chem. A* **2007**, *111*, 3110−3123.
(79) Poater, J.; Bofill, J. M.; Alemany, P.; Sola, M. *J. Org. Chem.* **2006**, *71*, 1700−1702.
(80) Munoz-Castro, A. *Chem. Phys. Lett.* **2011**, *517*, 113−115.
(81) Clever, H. L. *Krypton, Xenon, and Radon: Gas Solubilities*; Pergamon Press: Oxford, 1979.
(82) Zhang, X.; Lin, Y.; Gillies, R. J. *J. Nucl. Med.* **2010**, *51*, 1167−1170.
(83) Etzerodt, T. P.; Trier, S.; Henriksen, J. R.; Andresen, T. L. *Soft Matter* **2012**, *8*, 5933−5939.

DOI: 10.1021/jacs.5b01938
J. Am. Chem. Soc. 2015, 137, 5542−5548